Pharmacological Inhibition of Pleckstrin Homology Domain Leucine-Rich Repeat Protein Phosphatase Is Neuroprotective: Differential Effects on Astrocytes[S]

Travis C. Jackson, Jonathan D. Verrier, Tomas Drabek, Keri Janesko-Feldman, Delbert G. Gillespie, Thomas Uray, Cameron Dezfulian, Robert S. Clark, Hülya Bayir, Edwin K. Jackson, and Patrick M. Kochanek

University of Pittsburgh School of Medicine, Department of Critical Care Medicine, Safar Center for Resuscitation Research (T.C.J., P.M.K., H.B., R.S.C, K.J.F., C.D., T.U.) and Department of Pharmacology and Chemical Biology (J.D.V., D.G.G., E.K.J.),University of Pittsburgh School of Medicine, Pittsburgh, Pennsylvania; and Department of Anesthesiology, Presbyterian Hospital (T.D.), Pittsburgh, Pennsylvania

Received May 29, 2013; accepted September 10, 2013

ABSTRACT

Pleckstrin homology domain and leucine-rich repeat protein phosphatase 1 (PHLPP1) inhibits protein kinase B (AKT) survival signaling in neurons. Small molecule pan-PHLPP inhibitors (selective for PHLPP1 and PHLPP2) may offer a translatable method to induce AKT neuroprotection. We tested several recently discovered PHLPP inhibitors (NSC117079 and NSC45586; benzoic acid, 5-[2-[4-[2-(2,4-diamino-5-methyl-phenyl)diazenyl]phenyl]diazenyl]-2-hydroxy-,sodium salt.) in rat cortical neurons and astrocytes and compared the biochemical response of these agents with short hairpin RNA (shRNA)-mediated PHLPP1 knockdown (KD). In neurons, both PHLPP1 KD and experimental PHLPP inhibitors activated AKT and ameliorated staurosporine (STS)-induced cell death. Unexpectedly, in astrocytes, both inhibitors blocked AKT activation, and NSC117079 reduced viability. Only PHLPP2 KD mimicked PHLPP inhibitors on astrocyte biochemistry. This suggests that these inhibitors could have possible detrimental effects on astrocytes by blocking novel PHLPP2-mediated prosurvival signaling mechanisms. Finally, because PHLPP1 levels are reportedly high in the hippocampus (a region prone to ischemic death), we characterized hippocampal changes in PHLPP and several AKT targeting prodeath phosphatases after cardiac arrest (CA)-induced brain injury. PHLPP1 levels increased in rat brains subjected to CA. None of the other AKT inhibitory phosphatases increased after global ischemia (i.e., PHLPP2, PTEN, PP2A, and PP1). Selective PHLPP1 inhibition (such as by shRNA KD) activates AKT survival signaling in neurons and astrocytes. Nonspecific PHLPP inhibition (by NSC117079 and NSC45586) only activates AKT in neurons. Taken together, these results suggest that selective PHLPP1 inhibitors should be developed and may yield optimal strategies to protect injured hippocampal neurons and astrocytes— namely from global brain ischemia.

Introduction

Pleckstrin homology domain and leucine-rich protein phosphatases (PHLPPs) are ubiquitous serine/threonine phosphatases. Two PHLPP isoforms have been identified (PHLPP1 and PHLPP2). Furthermore, there are two PHLPP1 splice variants (PHLPP1α and PHLPP1β/suprachiasmatic nucleus circadian oscillatory protein). PHLPP1β/suprachiasmatic nucleus circadian oscillatory protein was first isolated from rat suprachiasmatic nucleus (Shimizu et al., 1999). Shortly thereafter PHLPP1α and PHLPP2 were discovered (Gao et al., 2005; Brognard et al., 2007). AKT is a key substrate of PHLPPs. Both isoforms inhibit AKT by dephosphorylation of Ser473, which induces cell death in cancer cells. PHLPP1 selectively targets/inhibits the AKT2 and AKT3 isoforms. PHLPP2 selectively targets/inhibits the AKT1 and AKT3 isoforms (Gao et al., 2005; Brognard et al., 2007). PHLPP1 inhibits AKT in neurons and astrocytes, but it is currently unknown if PHLPP2 serves similar functions in these cells.

AKT protects neurons from injury and stress and is a promising neurotherapeutic to treat brain ischemia (Fukunaga and

ABBREVIATIONS: AKT, protein kinase B; ANOVA, analysis of variance; CA, cardiac arrest; CMV, cytomegalovirus; CNS, central nervous system; DIV, day in vitro; DMEM, Dulbecco's modified Eagle's medium; DMSO, dimethylsulfoxide; ERK, extracellular regulated kinase; FBS, fetal bovine serum; IGF-1, insulin like growth factor-1; KD, knockdown; KO, knockout; LRR, leucine-rich repeat domain; MEK, mitogen-activated protein kinase kinase; NSC45586, benzoic acid,5-[2-[4-[2-(2,4-diamino-5-methylphenyl)diazenyl]phenyl]diazenyl]-2-hydroxy-,sodium salt. PHLPP, Pleckstrin homology domain and leucine rich repeat protein phosphatase; PP1, protein phosphatase 1; PP2A, protein phosphatase 2A; PP2C, protein phosphatase 2C domain; PTEN, phosphatase and tensin homolog; SD, Sprague-Dawley; STS, staurosporine; VF CA, ventricular fibrillation cardiac arrest.

Kawano, 2003; Luo et al., 2003; Jo et al., 2012). Recent studies confirm that PHLPP1 promotes CNS injury by inhibiting AKT. PHLPP1 KD in HT22 cells (an immortalized hippocampal neuron-derived cell line) activated AKT and protected against oxygen-glucose deprivation injury (Chen et al., 2013). In addition, PHLPP1 (−/−) KO mice had elevated AKT and were protected from experimental stroke induced by middle cerebral artery occlusion. Pretreatment with an AKT inhibitor completely prevented the protective phenotype (Chen et al., 2013).

PHLPP1 also inhibits extracellular regulated kinase (ERK). However, ERK and AKT are not regulated by the same mechanism. AKT is directly dephosphorylated by the protein phosphatase 2C (PP2C) domain in PHLPP1 (Gao et al., 2005). In contrast, ERK is indirectly inhibited by the PHLPP1 leucine-rich repeat (LRR) domain. Specifically, in neurons, the upstream GTPase K-RAS stimulates ERK phosphorylation. PHLPP1 binds to K-RAS (via its LRR domain) and prevents activation of the Ras-Raf-MEK-ERK cascade, which then prevents ERK phosphorylation (Shimizu et al., 2003). Thus, different PHLPP1 mechanisms inhibit AKT and ERK. The manner (or method) in which PHLPP1 is therapeutically targeted affects kinase activation. Total protein KD (e.g., by shRNAs) inhibits all functional domains (including the PP2C and LRR) causing both AKT and ERK to activate (Jackson et al., 2010). In contrast, selectively targeting the PP2C domain using small molecule inhibitors only activates AKT (Sierecki et al., 2010). The choice in PHLPP1 targeting strategy (for neuroprotection) may have important consequences on outcomes in global brain ischemia.

Studies show AKT activation, but not ERK, is neuroprotective after global brain ischemia. Pharmacological blockade of ERK reduced neuronal death in piglets injured by deep hypothermic circulatory arrest (Cho et al., 2004). In a similar study, ERK activation was elevated by low flow cardiopulmonary bypass-induced ischemia in piglets, which correlated with neuronal death in this model (Aharon et al., 2004). Finally, cardiac arrest (CA)-induced hippocampal CA1 death was associated with ERK activation in rats (Ozawa et al., 1999). In contrast, endogenous AKT activation was shown to be a key protective mechanism in the hippocampus after transient global brain ischemia in rats (Endo et al., 2006). Furthermore, therapeutic hypothermia (the standard of care therapy for some forms of global brain ischemia in humans) is less protective in AKT1 KO mice (Beiser et al., 2010).

Experimental pan-PHLPP inhibitors including NSC117079 and NSC45586 were recently identified (Sierecki et al., 2010). These agents reportedly (selectively) target the PP2C phosphatase domain of PHLPP1 and PHLPP2 (i.e., the key site of AKT dephosphorylation and inactivation). In kidney (COS-7) and colon (HT29) cells, PHLPP inhibitors potentiate AKT activation but not ERK (Sierecki et al., 2010). These compounds may offer a translatable therapy to target pro-death PHLPP1 mechanisms in global brain ischemia. However, they must first be tested in primary CNS cells. Here we investigate if several PHLPP inhibitors (NSC117079 and NSC45586) selectively activate AKT in primary rat cortical neurons and astrocytes. Furthermore, because PHLPP1 is abundant in the ischemia vulnerable CA1 hippocampal subregion and it inhibits AKT activation in primary

hippocampal neurons, we explored if key brain phosphatases (including PHLPP1 and PHLPP2) increased in the rat hippocampus after CA (Jackson et al., 2009, 2010).

Materials and Methods

Animals

Adult and embryonic Sprague-Dawley (SD) rats were purchased from Charles River (Wilmington, MA). All procedures were approved by the Institution Animal Care and Use Committee of University of Pittsburgh.

Experimental Compounds and Reagents

NSC117079 and NSC45586 were generously provided at request from the National Cancer Institute Division of Cancer Treatment and Diagnosis. Compounds were provided in opaque glass vials. PHLPP inhibitors were dissolved in 100% dimethylsulfoxide (DMSO) and subsequently added directly to Neurobasal media (Life Technologies. Grand Island, NY) at desired final concentrations. All final DMSO concentrations were <2%. Within each experiment, all groups received equal concentrations of DMSO. Recombinant IGF-1 protein was purchase from PeproTech (Rocky Hill, NJ). Staurosporine was purchased from Tocris (Bristol, UK) and dissolved in 100% DMSO.

Cell Culture

Cortical neurons were harvested from E17-E19 SD rat embryos using our previously published methods that yielded ∼95% pure neuronal populations (Jackson et al., 2010). Neuron populations were gender mixed (i.e., originating from both male and female tissues). In brief, embryonic brains were isolated, trypsinized, triturated, and seeded onto either 6-well or 96-well poly-D-lysine culture plates (BD Biosciences, San Jose, CA). Neurons were grown in Neurobasal media (Life Technologies) containing B27 supplement and maintained by 1/2 media exchange every 3–4 days. Cytosine arabinoside was added at day in vitro (DIV) 3 to prevent glial proliferation. Studies show that isolated embryonic neural cells rapidly adopt adult morphology and functional characteristics in culture (Brewer et al., 1993; Lin et al., 2002). All experiments were performed between DIV6 and 12. Astrocytes were harvested using a previously published protocol (Verrier et al., 2011). In brief, postnatal day 1–2 SD rat pup brains (sex mixed) were isolated, trypsinized, triturated, and seeded onto T-75 culture flasks. Cells were grown to 80–90% confluence in DMEM/F12/10% fetal calf serum. After 1–2 propagations, astrocytes were seeded onto 6-well plates and grown to confluence for PHLPP KD experiments.

Viability Assay

CellTiterBlue. Neurons were injured by STS using previously reported methods (Jackson et al., 2013). Briefly, cells were seeded onto 96-well plates at high density (1.5×10^5/well). At DIV10–12 maintenance growth media was replaced with 100 μl of drug treatment media (i.e., 1/2 conditioned growth media + 1/2 fresh Neurobasal/B27) containing different concentrations of STS with or without experimental PHLPP inhibitors. After a 24-hour injury period, 20 μl CellTiterBlue reagent (Promega, Madison, WI) was added to each well. Viable neurons metabolize the CellTiterBlue reagent, and the resulting color change is detected using a α-Fusion Plate Reader (Packard/PerkinElmer, Waltham, MA). For astrocyte studies, cells were used at third passage and seeded onto poly-D-lysine coated 96-well assay plates. Astrocytes were grown to confluence over ∼48 hour. Confluent monolayers were treated with increasing doses of NSC45586 or NSC117079 for 24 hours (prepared in DMEM/F12/10% FBS; 100 μl/well). After 24-hour drug treatments, cells were

incubated with 20 μl of CellTiterBlue reagent for 30 minutes to 1 hour and analyzed on a plate reader.

Calcein AM. Embryonic neurons were seeded onto Laboratory-Tek II 8-well glass chamber slides at a density of 400,000 cells/well (Thermo Fisher Scientific, Pittsburgh, PA). Neurons were maintained in culture by half of media replacement every 3 days. Cytosine arabinoside was excluded in these experiments to allow astrocyte proliferation (i.e., mixed neuron/astrocyte cultures). At DIV8, DMSO or 50 nM STS ± 200 μM NSC45586 was added to cultures for 24 hours. On DIV9 neurons were washed twice with DPBS and subsequently incubated with 2 μM calcein AM (Life Technologies) for ~10 minutes. Live cell images (10× objective) were immediately captured using a fluorescent microscope. Images were collected from two different wells for each treatment group. Random images from each well were selected for analysis. Two boxes of equal size were randomly drawn in each image, in Photoshop, and green (live cells) counted (a white spot placed next to each cell to ensure counting accuracy). Total cell counts were averaged and graphed. For astrocyte studies, cells were seeded onto glass chamber slides. Approximately 48 hours later, astrocytes were incubated with NSC45586 or NSC117079 at the indicated concentrations for 24 hours. Cells were washed twice with DPBS and incubated with 2 μM calcein AM for ~10 minutes, and images were captured using a florescent microscope.

Viral Production

Lentiviral vectors were produced using the pLK0.1 plasmid system, which contains a puromycin selection marker and a CMV expression promoter. In brief, viral packaging plasmids + pLKO.1 vector (with a subcloned PHLPP1 or PHLPP2 shRNA) were cotransfected into human embryonic kidney 293FT cells and grown on T-225 flasks. Virus-enriched growth media (DMEM/10% FBS) was collected 24 and 48 hours post-transfection. Media were passed through a 0.45-μm filter top system to remove cellular debris. Viral particles were concentrated first by centrifuging media through a Centricon Plus 70 filter unit (Millipore, Billerica, MA) and then a final spin in an ultracentrifuge (1.5 hour/24,000 rpm/4°C). The pellet (containing high titer virus) was resuspended in 25 μl of DMEM and portioned into aliquots into sterile vials. Virus was stored at −80°C until use. Neurons were transduced with virus on the day of isolation at a multiplicity of infection 30. Astrocytes were transduced at a multiplicity of infection 100 and subsequently puromycin selected. Cells were transduced with either nontargeting control or PHLPP-targeting vectors. We used the PHLPP1 targeting shRNA clones ID TRCN0000081362 and TRCN0000081359 (as previously published in neurons) and a PHLPP2 targeting shRNA clone ID TRCN0000082660 (Open Biosystems/Thermo Fisher Scientific, Pittsburgh, PA).

Western Blot

Cell extracts or brain tissues were harvested in radioimmunoprecipitation assay buffer prepared with EDTA, protease inhibitors, and phosphatase inhibitors. Samples were sonicated 20–30 seconds and spun with a tabletop ultracentrifuge (10 minutes/16,000 rpm/4°C). Protein concentrations were determined using the bicinchoninic acid assay (Pierce, Rockford, IL). Twenty micrograms protein per sample was loaded onto either 7.5 or 4–15% gradient precast SDS-PAGE TGX gels (BioRad, Hercules, CA) and run for 2 hours at 200 V. Electrophoresed proteins were transferred to polyvinyldifluoride membrane (~1 hour/100 V/4°C). Blots were blocked in 7.5% milk for 1 hour. Primary antibodies were diluted in Tris-buffered saline + Tween-20. Phospho-AKT473, AKT total, phospho-ERK1/2, ERK1/2 total, α-tubulin, and glyceraldehyde 3-phosphate dehydrogenase were purchased from Cell Signaling Technology (Danvers, MA). PHLPP1 and PHLPP2 antibodies were purchased from Bethyl Laboratories (Montgomery, TX). Blots were incubated overnight at 4°C with primary antibodies, washed with Tris-buffered saline, incubated with

goat anti-mouse/rabbit secondary antibodies for 2 hours, washed again, and developed using the ECL-2 Plus Western blot detection reagent (Pierce). Films were exposed to blots in a dark room, developed, and scanned for data analysis. Densitometry was obtained using UN-SCAN-IT software (Silk Scientific, Orem, UT). Graphs were built using PRISM software (GraphPad Software Inc., La Jolla, CA). Data were analyzed using Number Cruncher Statistical System (NCSS) statistical software (Saugus, MA).

Ventricular Fibrillation Cardiac Arrest-Induced Brain Injury

We made minor modifications to an established model of rat VF CA that reproducibly produces ≥70% hippocampal CA1 cell death at 1 week as described previously by Janata et al. (2013). Adult SD rats (350–400 g) were anesthetized using 4% isoflurane in oxygen. A 14-gauge intravenous cannula was inserted into the trachea, and animals were connected to a ventilator (30% oxygen). Isoflurane was decreased to 2% (i.e., maintenance dose). Physiologic measurements were continually recorded throughout the procedure. These included electrocardiography, rectal/tympanic temperatures, and arterial and venous blood pressures (via fluid-filled catheters). A 12 V/50 Hz alternating current was continually applied via a jugular electrode pacing catheter over a 2-minute period to induce VF. CA was verified by electrocardiography (heart rate) and arterial blood pressure recordings. After a total of 6 minutes VF CA, cardiopulmonary resuscitation was initiated with chest compressions, mechanical ventilation (100% oxygen), epinephrine (0.02 mg/kg i.v.), and bicarbonate (1 mEq/kg i.v.). After 2 minute of cardiopulmonary resuscitation animals were defibrillated (5 J) and recovered for 1 hour. Sham-treated animals received the same anesthesia and surgical manipulations but were not subjected to VF CA. Sham- and VF CA-injured rats were killed 24 hours later by decapitation under deep anesthesia and brains were quickly isolated, and the hippocampi were dissected and snap-frozen in liquid nitrogen. Samples were stored at −80°C until homogenization for biochemical analysis of proteins.

Statistics

For dose-response studies AKT/ERK levels were normalized using glyceraldehyde 3-phosphate dehydrogenase expression, and intrablot values were set to the maximum number (i.e., for interblot comparisons). All data were graphed using PRISM (GraphPad Software Inc.) and analyzed with either analysis of variance (ANOVA) or unpaired t test using NCSS statistical software. For ANOVA, the Newman-Keuls multiple-comparison post hoc test was used to analyze group differences. Data were significant at $P < 0.05$. Graphs show mean + S.E.M.

Results

PHLPP1 Regulates AKT and ERK in Rat Primary Cortical Neurons

We previously reported that PHLPP1 KD activates AKT/ERK in rat primary hippocampal neurons (Jackson et al., 2010). Cortical neurons were employed to study PHLPP signaling in this study. Therefore we first verified that PHLPP1 KD also activates AKT/ERK in rat primary cortical neurons. Cells were transduced with lentivirus to deliver either control (i.e., nontargeting) or PHLPP1 targeting shRNAs at time of plating. On day in vitro 6 (DIV6) protein extracts were collected for Western blots. Consistent with prior observations, PHLPP1 KD potently increased basal AKT and ERK phosphorylation in cortical neurons (Fig. 1A). We next tested if PHLPP1 KD protected cortical neurons from injury. Cells were seeded onto a 96-well plate and transduced with control or PHLPP1 KD vectors. Neuron viability was significantly higher 24 hours after STS injury in the PHLPP1 KD group (Fig. 1B).
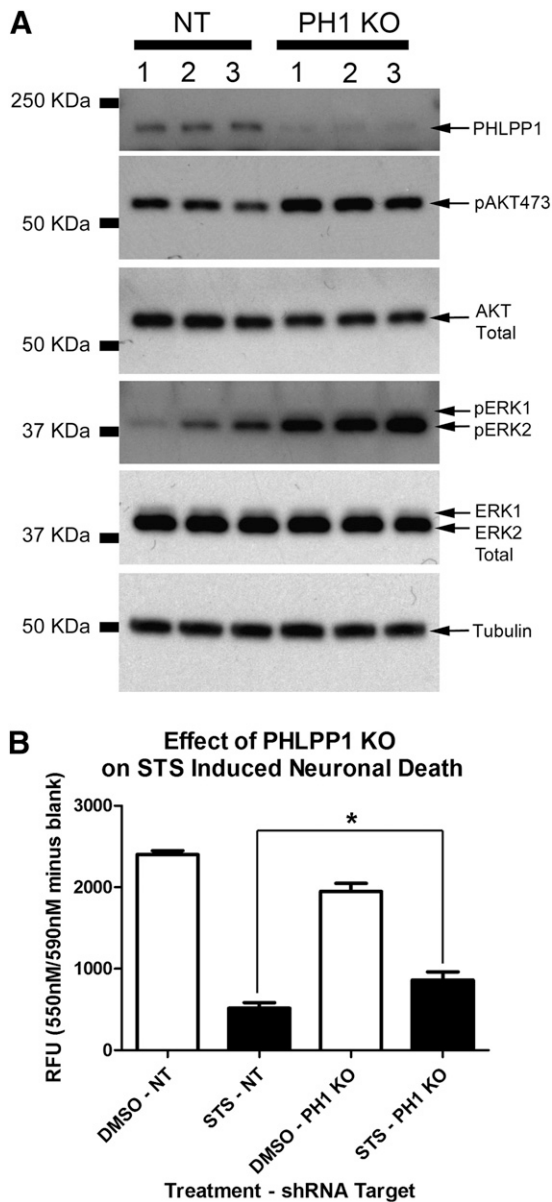
Fig. 1. PHLPP1 KO protects cortical neurons from STS injury. (A) Primary rat cortical neurons were grown onto six-well plates and transduced with control (NT) or PHLPP1 KO viral vectors. Western blots confirm increased pAKT473 and pERK1/2 after PHLPP1 KO; experiment was performed in triplicate. (B) Primary rat cortical neurons were seeded onto a 96-well plate and injured 24 hours with 150 nM STS. PHLPP1 KO significantly increased 24 hour viability (expressed as relative fluorescent units; RFU) compared with controls ($n = 8$ replicates/group). Data were analyzed by ANOVA and Newman-Keuls multiple comparison post hoc test. *$P < 0.05$. Graphs show mean + S.E.M.

PHLPP-PP2C Inhibitors Selectively Raise Basal AKT in Neurons

Sierecki et al. (2010) showed that a 24-hour serum starvation (to investigate basal signaling conditions) followed by 35-minute drug treatment with NSC117079 or NSC45586 activated basal AKT in COS-7 cells. We adopted a similar treatment protocol for primary rat cortical neuron experiments. Neurobasal maintenance growth medium was replaced with fresh Neurobasal medium (without B27 supplement) to give a 2-hour supplement starvation. PHLPP inhibitors were diluted to final concentration in unsupplemented Neurobasal media
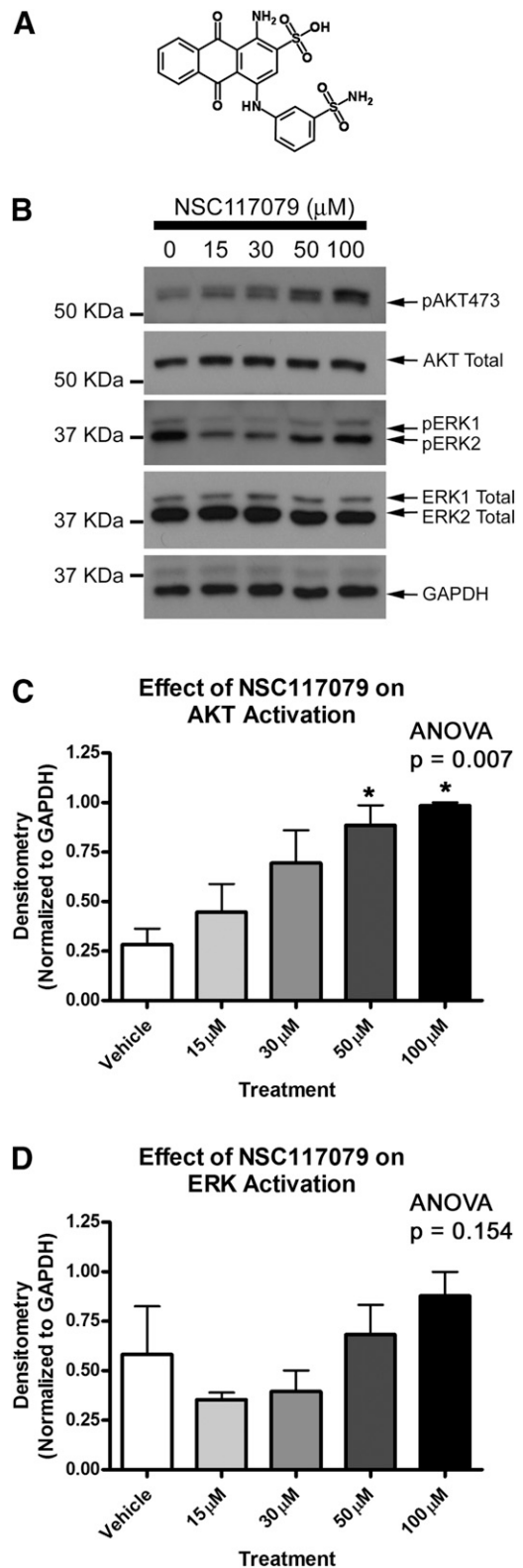

Fig. 2. PHLPP inhibitor NSC117079 activates neuronal AKT. (A) Image showing two-dimensional structure of NSC117079. Primary rat cortical neurons were grown onto six-well plates, supplement starved 2 hours, and treated with increasing doses of NSC117079 (experiments performed in triplicate). (B) Representative blot showing elevated phospho-AKT473 levels at increasing drug doses. (C) Semiquantitative densitometry showing elevated pAKT473 ($n = 3$/group). (D) Semiquantitative densitometry showing that pERK1/2 is not significantly altered by drug treatments ($n = 3$/group). Data were analyzed by ANOVA and Newman-Keuls multiple comparison post hoc test. *Significant post hoc difference ($P < 0.05$) compared with DMSO control group. Graphs show mean + S.E.M.
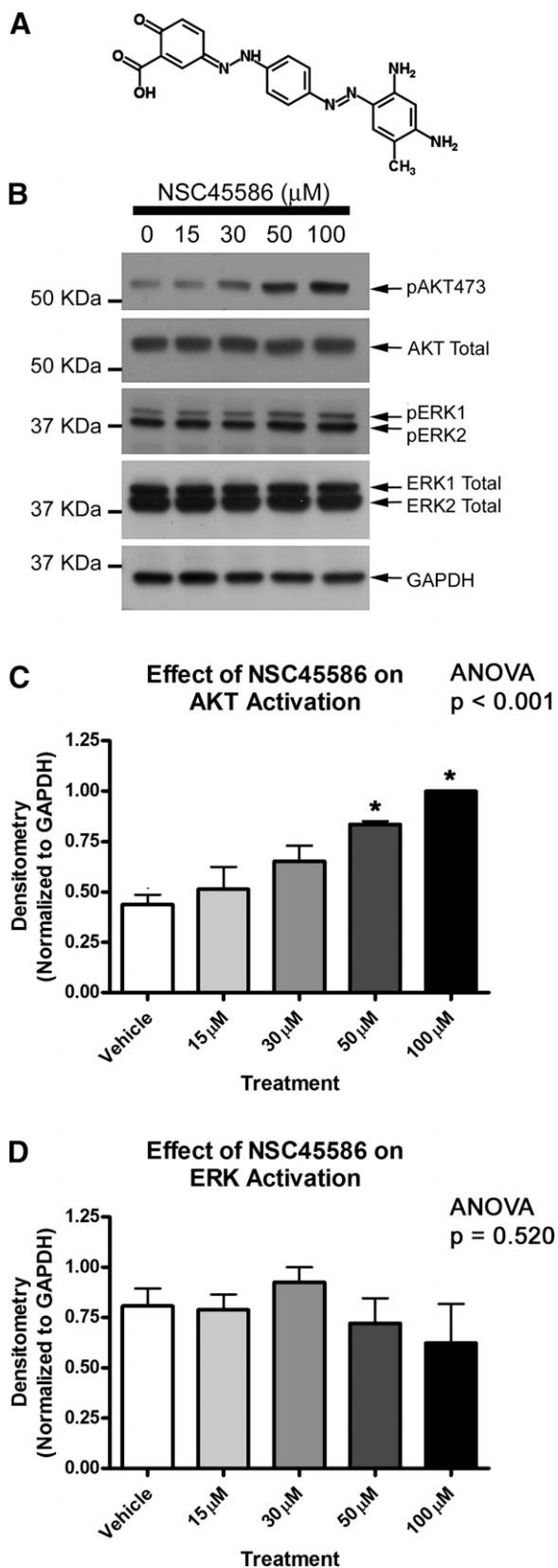
and incubated on neurons for 35 minutes. PHLPP inhibitors increased basal neuronal AKT activation in a dose-dependent manner (Figs. 2 and 3). NSC117079 showed a tendency to elevate ERK phosphorylation (Fig. 2D) but NSC45586 did not (Fig. 3D).

Our previous work showed that neuronal PHLPP1 KD potentiates IGF-1 induced AKT phosphorylation, suggesting that PHLPP1 also inhibits the upper threshold of AKT activation (Jackson et al., 2010). We next tested if NSC45586 potentiated IGF-1 induced AKT phosphorylation. Neurons were supplement starved 2 hours and subsequently treated for 35 minutes with 50 ng/ml IGF-1 in the absence (i.e., 0 μM NSC45586) or presence of increasing NSC45586 doses. NSC45586 dose dependently augmented IGF-1-induced AKT activation except at the highest concentration (Fig. 4). The optimal concentration was 50 μM. At this dose pAKT473 maximally increased (Fig. 4B) but pERK was unaffected compared with controls (Fig. 4C). Surprisingly NSC117079 did not potentate AKT activation. Rather it dose dependently inhibited AKT activation in the presence of IGF-1 and altered AKT total levels (Supplemental Fig. 1).

PHLPP Inhibitors Are Neuroprotective

We next tested if PHLPP inhibitors rescued neurons from cell death. Primary rat cortical neurons were seeded onto 96-well assay plates. Neurons were injured by 24-hour treatment with staurosporine (STS). All groups treated with STS showed a significant reduction in viability compared with respective uninjured controls (white bars). Furthermore, a 35-minute pretreatment with NSC45586 or NSC117079 failed to augment cell survival compared with injured (STS only) control (Fig. 5D). In contrast, 24-hour cotreatment with NSC117079 or NSC45586 significantly increased viability compared with injured (STS only) controls (Fig. 5, A–C). The neuroprotective effects were reproducible and more pronounced at lower STS injury levels (Fig. 5A). CellTiterBlue viability results were supported by live cell counting. NSC45586 (200 μM) increased the number of live cells, as measured by calcein AM fluorescence, after 24 hour 50 nM STS injury (Supplemental Fig. 2).

NSC45586 (50 μM) only moderately protected against STS injury as measured by CellTiterBlue viability. However, it was the optimal concentration that induced AKT survival signaling in dose-response studies. Of note, acute AKT dose-response studies were done under albumin-free treatment conditions (i.e., with unsupplemented Neurobasal media). We observed that 50 μM NSC45586 rapidly bound bovine serum albumin (2.5 g/l) in basal culture media (Supplemental Fig. 4). Albumin-containing B27 supplement was required for 24-hour culture maintenance after STS injury and may have interfered with AKT activation at low dose NSC45586.

PHLPP Inhibitors Reduce AKT and ERK Activation in Astrocytes

We next tested PHLPP inhibitors on primary rat astrocytes under albumin-free treatment conditions (after a 2-hour

Fig. 3. PHLPP inhibitor NSC45586 activates neuronal AKT. (A) Image showing two-dimensional structure of NSC45586. Primary rat cortical neurons were grown onto six-well plates, supplement starved 2 hours, and treated with increasing doses of NSC45586 (experiments performed in triplicate). (B) Representative blot showing elevated pAKT473 levels at increasing drug doses. (C) Semiquantitative densitometry showing elevated pAKT473 (n = 3/group). (D) Semiquantitative densitometry showing that pERK1/2 is not significantly altered by drug treatments (n = 3/group). Data were analyzed by ANOVA and Newman-Keuls multiple comparison post hoc test. *Significant post hoc difference (P < 0.05) compared with DMSO control group. Graphs show mean + S.E.M.
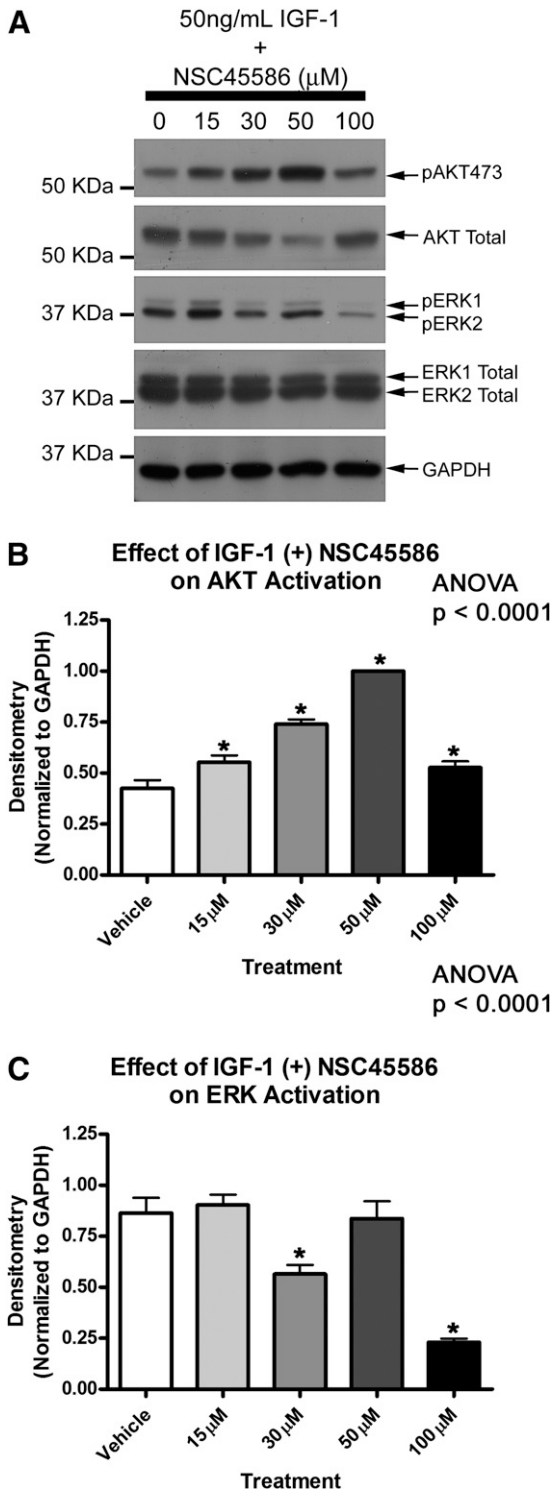
Fig. 4. PHLPP inhibitor NSC45586 potentiates IGF-1-induced AKT Activation. (A) Primary rat cortical neurons were grown onto 6-well plates, supplement starved 2 hours, and treated with 50 ng/ml IGF-1 in the absence (control) or presence of increasing NSC45586 doses (experiments performed in triplicate). Representative blot showing elevated pAKT473 levels and altered pERK levels at different drug doses. (B) Semiquantitative densitometry showing NSC117069 potentiates IGF-1-induced pAKT473 levels (n = 3/group). (C) Semiquantitative densitometry showing that in the presence of IGF-1, 30 and 100 μM NSC45586 significantly decreases pERK1/2 (n = 3/group). Data were analyzed by ANOVA and Newman-Keuls multiple comparison post hoc test. *Significant post hoc difference ($P < 0.05$) compared with DMSO control group. Graphs show mean + S.E.M.

serum starvation). The optimal AKT activating dose, empirically identified for neurons (50 μM), was tested in astrocytes. A 35-minute treatment with 50 μM NSC45586 or NSC117079 unexpectedly inhibited basal AKT and ERK phosphorylation (Fig. 6, A–D). NSC45586 more potently inhibited AKT compared with NSC117079 (Fig. 6C). Alternatively, NSC117079 more potently inhibited ERK compared with NSC45586 (Fig. 6D). We next tested whether NSC45586 or NSC117079 reduced basal astrocyte viability. PHLPP inhibitors were prepared in fresh astrocyte growth media (DMEM/F12/10% FBS) and incubated for 24 hours. NSC117069 dose dependently inhibited basal viability as measured by CellTiterBlue metabolism (Fig. 6E). In contrast, NSC45586 did not reduce viability across the 24-hour period (Fig. 6F). Calcein AM florescence in astrocytes also revealed changes consistent with the CellTiterBlue results. NSC117079 induced a dose-dependent loss of astrocytes as indicated by thinning of calcein AM fluorescence. Furthermore, NSC117079 altered cell morphology. Large diffuse cell bodies are typical of astrocyte monolayers (DMSO group). NSC117079 altered cell structure to an elongated shape with increasing drug concentrations (Supplemental Fig. 3).

PHLPP1 and PHLPP2 Differentially Regulate AKT and ERK in Astrocytes

To better understand the biochemical changes induced by PHLPP inhibitors in astrocytes, we next tested whether PHLPP1 or PHLPP2 KD could mimic the response. Primary rat astrocytes were transduced with lentivirus vectors, administered puromycin selection over 72 hours (i.e., to kill nontransduced cells) and harvested for protein analysis under 10% FBS growth conditions. Similar to observations in neurons, PHLPP1 KD activated AKT in astrocytes (Fig. 7, A and B). However, ERK was unaffected by PHLPP1 KD (Fig. 7, A and C). We next tested whether PHLPP2 KD mimicked the effect of PHLPP inhibitors on astrocytes. PHLPP2 KD tended to decrease both AKT and ERK activation (although the results did not reach statistical significance; Fig. 7, A, D, and E). The potential roles of PHLPP1 and PHLPP2 in neurons/astrocytes are illustrated in Fig. 7F.

Effect of VF CA Induced Ischemia on AKT/ERK Targeting Phosphatases in the Hippocampus

It remains unclear what is the optimal in vivo PHLPP targeting strategy for brain injury (i.e., selective PHLPP1 inhibitors versus selective PHLPP2 inhibitors versus pan-PHLPP inhibitors). The hippocampus is a key brain region damaged by ischemia, particularly in transient global brain ischemia, as produced by CA and resuscitation in humans (Horstmann et al., 2010). Ischemia-induced changes in hippocampal PHLPP levels have not been explored. We tested whether PHLPPs and their target kinases (AKT/ERK) were altered after global brain ischemia using a clinically relevant rat model of VF CA that we previously showed displays robust neuronal death in CA1 hippocampus (Janata et al., 2013). Induction of CA was confirmed by monitoring heart rate (Supplemental Fig. 5) and mean arterial pressure (Supplemental Table 2). Physiologic parameters from the rats exposed to CA and shams are provided in Supplemental Table 1. Hippocampal pAKT and pERK were robustly increased above noninjured levels 24 hours after a 6-minute
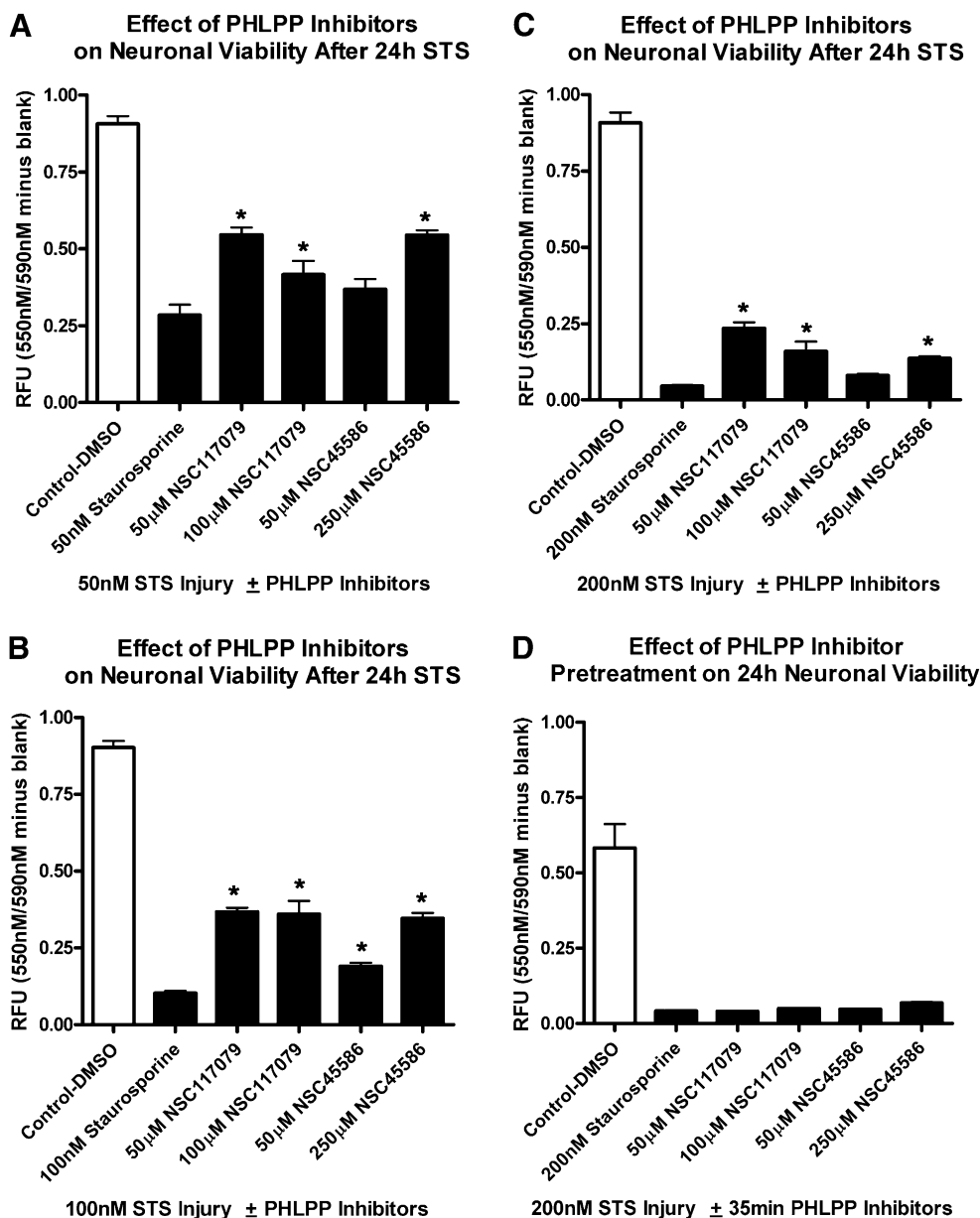
A

Effect of PHLPP Inhibitors
on Neuronal Viability After 24h STS

50nM STS Injury ± PHLPP Inhibitors

C

Effect of PHLPP Inhibitors
on Neuronal Viability After 24h STS

200nM STS Injury ± PHLPP Inhibitors

Fig. 5. PHLPP inhibitors protect cortical neurons from STS injury. Primary rat neurons were seeded onto 96-well plates. (A–C) Cells were coincubated 24 hours with PHLPP inhibitors and 50 nM STS (A), 100 nM STS (B), or 200 nM STS (C). Neuronal viability was measured by CellTiterBlue metabolism 24 hours later. (D) Cells were given a 35-minute pretreatment with PHLPP inhibitors. Drugs were removed and replaced with media containing 200 nM STS. Viability was measured by CellTiterBlue metabolism 24 hours later. Experiments were performed in replicates; $n = 7$ for the 250 μM NSC45586 groups in (B and C) and $n = 8$ for all other groups. White bars show uninjured control groups treated with DMSO only. Black bars show groups treated with STS for 24 hours. Data were analyzed by ANOVA and Newman-Keuls multiple comparison post hoc test. *Significant post hoc difference ($P < 0.05$) for PHLPP-inhibitor treated groups compared with injury (STS only) control. Graphs show mean + S.E.M.

B

Effect of PHLPP Inhibitors
on Neuronal Viability After 24h STS

100nM STS Injury ± PHLPP Inhibitors

D

Effect of PHLPP Inhibitor
Pretreatment on 24h Neuronal Viability

200nM STS Injury ± 35min PHLPP Inhibitors

VF CA (Fig. 8). Among five different brain phosphatases measured, only PHLPP1 significantly increased 24 hours after a 6-minute VF CA (Fig. 9, A and B). PHLPP2 levels did not change (Fig. 9, A and C). In contrast, three other phosphatases PTEN, PP1α, and PP2A all significantly decreased in the hippocampus 24 hours after a 6-minute VF CA (Fig. 9, A and D–F).

Discussion

PHLPP Inhibitors Are Promising New Neuroprotective Agents

Here we characterized two different PHLPP inhibitors (NSC117079 and NSC45586) in primary rat cortical neurons and astrocytes. These agents reportedly target the PP2C phosphatase domain (i.e., the AKT regulatory domain) in PHLPP1 and PHLPP2. They do not inhibit the PHLPP-LRR domain (which is involved in K-RAS/ERK regulation). Consistent with this understanding, in neurons, both compounds activated basal AKT and reduced STS-induced cell death. Neither drug significantly increased basal ERK activation. However, at higher doses (50–100 μM), NSC117079 tended to elevate ERK phosphorylation in neurons while NSC45586 did not. Therefore, NSC45586 affected neuronal AKT/ERK signaling in a manner consistent with a predicted (selective) PHLPP-PP2C inhibitor. We also compared the effect of PHLPP1 KD on cortical neuron biochemistry. PHLPP1 KD (non-selectively) inhibits all functional domains; including the LRR domain which regulates ERK inhibition. Therefore, as expected, PHLPP1 KD activated both AKT and ERK in neurons. Furthermore, PHLPP1 KD was neuroprotective.

Inhibiting PHLPP1 by selectively targeting the PP2C domain may be an optimal therapeutic strategy for some types of acute brain injury. Studies show that ERK activation
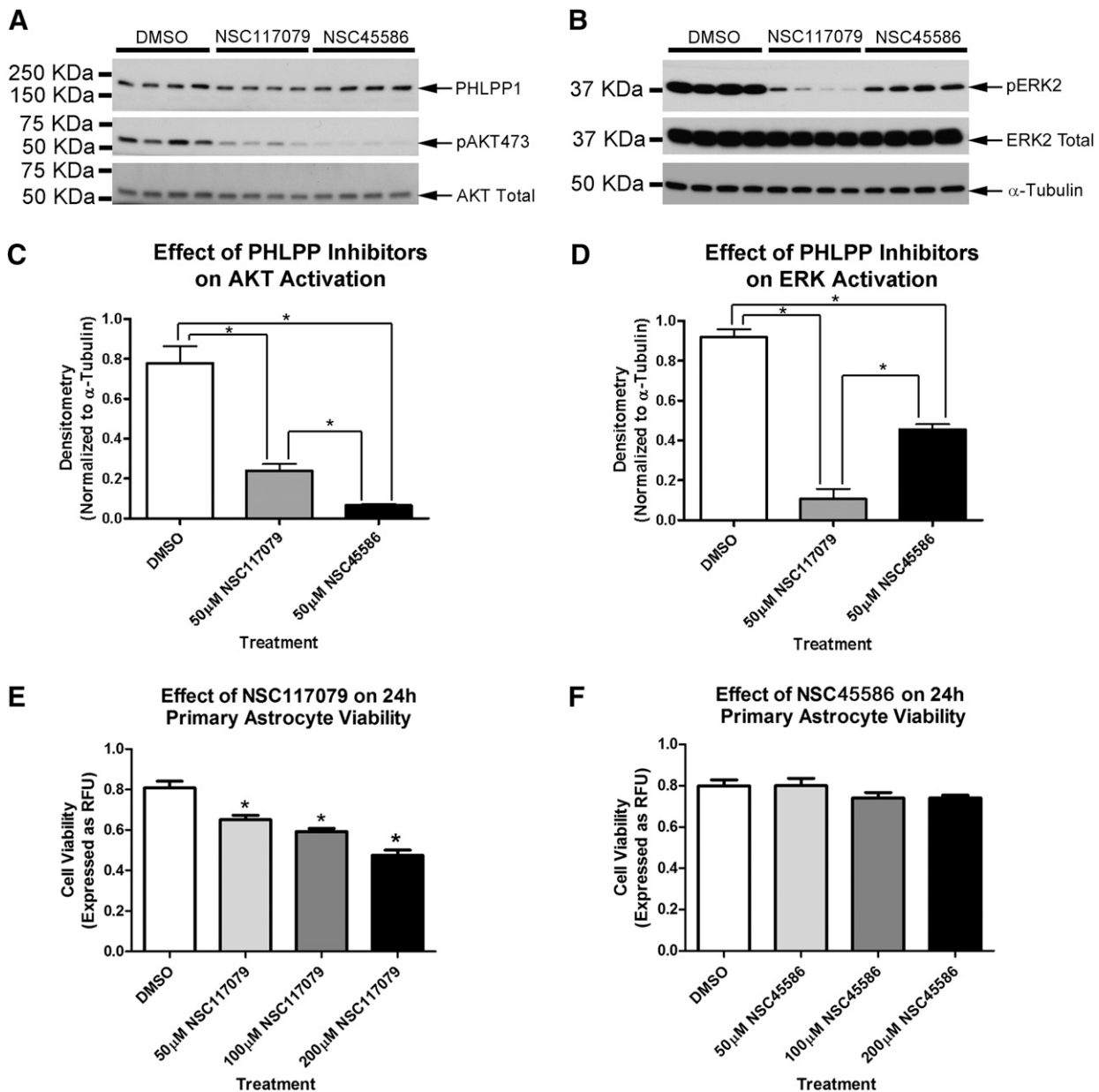
Fig. 6. PHLPP inhibitors inactivate AKT/ERK and alter basal viability in astrocytes. Primary rat astrocytes were grown to confluence on six-well plates. (A and B) Western blot shows 50 μM NSC117079 and 50 μM NSC45586 decrease AKT/ERK phosphorylation in astrocytes. Experiment performed in quadruplicate. (C and D) Semiquantitative densitometry showing that pAKT473 ($n = 4$/group) and pERK1/2 ($n = 4$/group) significantly decrease by treatment. (E and F) Only NSC117079 reduced basal viability in astrocytes after a 24-hour incubation ($n = 10$ replicates/bar). Data were analyzed by ANOVA and Newman-Keuls multiple comparison post hoc test. *$P < 0.05$. Graphs show mean + S.E.M. KDa, kilodalton.

promotes neuronal death and worsens neurologic outcomes in ischemic (Ozawa et al., 1999; Lu et al., 2010) and traumatic brain injury (Raghupathi et al., 2003; Clausen et al., 2004; Lu et al., 2005). PHLPP1 targeting strategies that decrease total protein levels may inadvertently promote cell death by freeing PHLPP1-LRR-mediated ERK inhibition (which in turn might induce deleterious ERK activation). PHLPP-PP2C inhibitors are thus potentially advantageous because they only activate AKT-mediated survival mechanisms. However, ERK activation may not be detrimental in all brain injury paradigms. PHLPP1 KO mice were recently shown to have reduced brain infarct volumes after stroke injury (Chen et al., 2013). Administering an AKT inhibitor before ischemia completely reversed the protective KO phenotype. Thus, in this study,

neuronal ERK activation (presumably upregulated in KOs) neither enhanced nor prevented neuroprotection in transgenic mice. To date, most studies have focused on the PHLPP1/AKT signaling axis. In addition, ERK activation may have beneficial effects on learning and memory independent of effects on neuronal death (Dash et al., 2002). More studies are needed to better understand the consequences of ERK activation (as it relates to PHLPP1 inhibition) in the context of ischemic brain injury.

Limitations of NSC45586 and NSC117079

Both of the PHLPP inhibitors tested in this study reduced death of primary neurons. However, our results also reveal
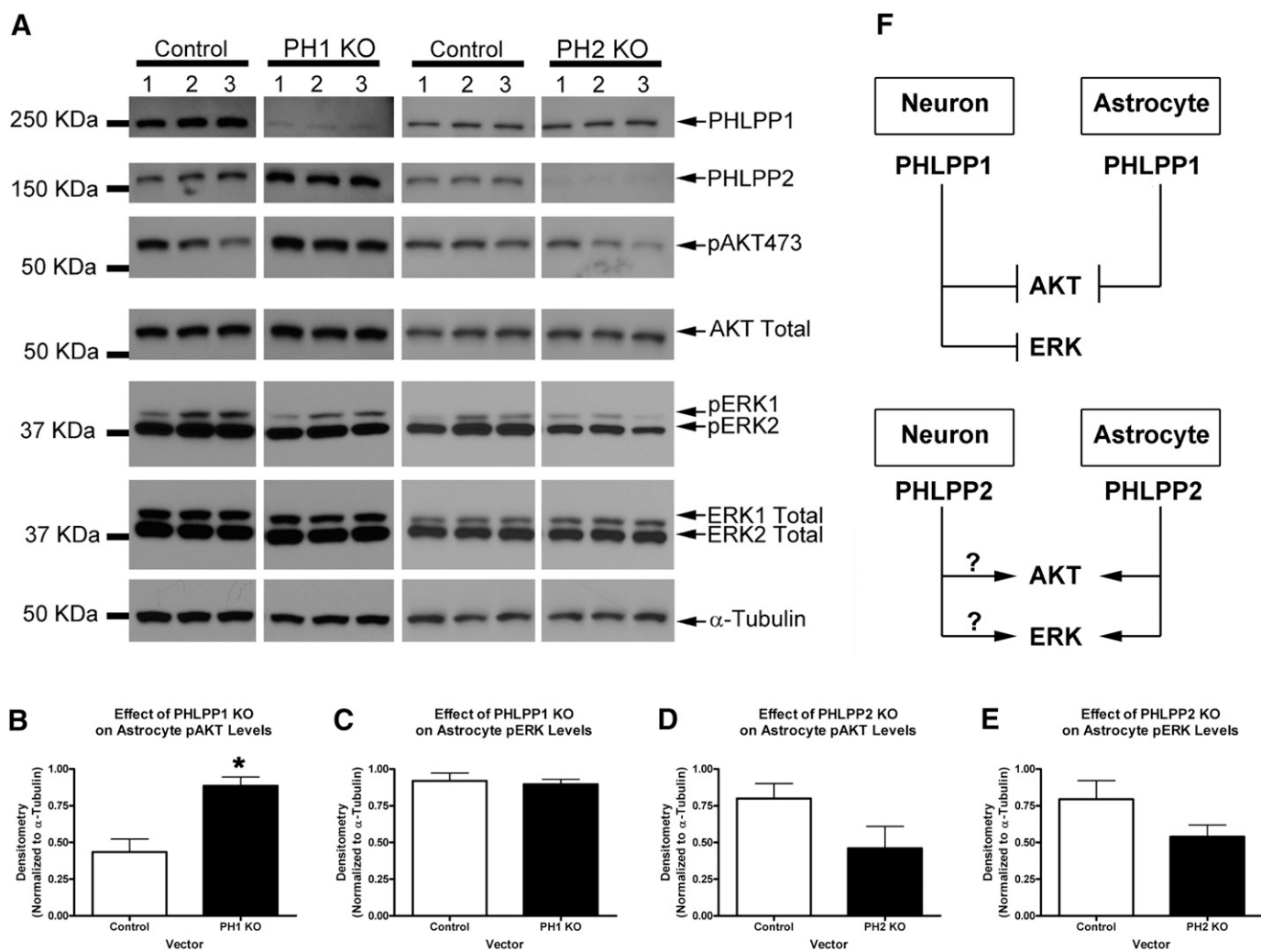
A

F

Fig. 7. Different roles of PHLPP isoforms in astrocytes. Astrocytes were transduced with PHLPP1 or PHLPP2 KO vectors and puromycin selected for 72 hours. Cells were harvested 24 hour later under growth conditions (DMEM/F12/10% fetal calf serum). (A) Western blots comparing the effect of PHLPP KO on biochemistry. Experiment performed in triplicate. (B) Semiquantitative densitometry showing that PHLPP1 KO compared with its respective control significantly increased pAKT473 (n = 3/group). (C) Semiquantitative densitometry showing that PHLPP1 KO did not alter pERK1/2 (n = 3/group). (D) Semiquantitative densitometry showing that PHLPP2 KO tended to decrease pAKT473 (n = 3/group). (E) Semiquantitative densitometry showing that PHLPP2 KO tended to decrease pERK1/2 (n = 3/group). (F) A schematic illustrating PHLPP signaling differences comparing neurons to astrocytes. Data were analyzed by unpaired t test. *$P < 0.05$. Graphs show mean + S.E.M. KDa, kilodalton.

some potential limitations of these compounds. NSC45586, which was the best PHLPP inhibitor in this study, avidly bound to bovine serum albumin. Protein binding might limit its use in vivo. This idea is supported by our in vitro studies. It took five times more NSC45586 (250 μM) to induce neuroprotection on the STS injury model (in the presence of B27 supplement, which contains albumin). However, NSC45586 induced maximal AKT activation at 50 μM in albumin-free experiments. Furthermore, our observations are consistent with Sierecki et al. (2010), who used 250 μM NSC45586 to activate AKT in cells maintained under 5% fetal bovine serum. Alternatively, under serum/albumin-free conditions, they reported that NSC45586 increased basal AKT phosphorylation with an IC_{50} of 70.6 μM. Thus, serum albumin binding may have hindered PHLPP antagonism in their experiments as well.

NSC117079 was also neuroprotective despite a less optimal biochemical profile; NSC11709 mildly upregulated ERK and blocked IGF-1-induced AKT activation at 50 and 100 μM.

Off-target effects may play a role. Sierecki et al. (2010) showed that 100 μM NSC117079 also inhibited protein phosphatase 1 (PP1) and protein phosphatase 2 Cα (PP2Cα) catalytic domains by $\sim$50%. Furthermore, NSC117079 was previously found to bind and modulate the G-protein $\beta\gamma$ subunit, IC_{50} 56 μM (Bonacci et al., 2006). G$\beta\gamma$ regulates PI3Kγ activation (Schwindinger and Robishaw, 2001), which can modulate the AKT/ERK pathways (Murga et al., 1998). Finally, NSC117079 may also bind neuraminidase (Mai et al., 2010), which regulates neuronal excitability and synaptogenesis (Isaeva et al., 2010). A literature search did not uncover any non–PHLPP targets for NSC45586.

PHLPP1 Inhibition in Neurons versus Astrocytes: Implications on Cytoprotection

The biochemical changes induced by PHLPP inhibitors were markedly different in astrocytes than neurons. In astrocytes, both inhibitors blocked AKT/ERK phosphorylation.
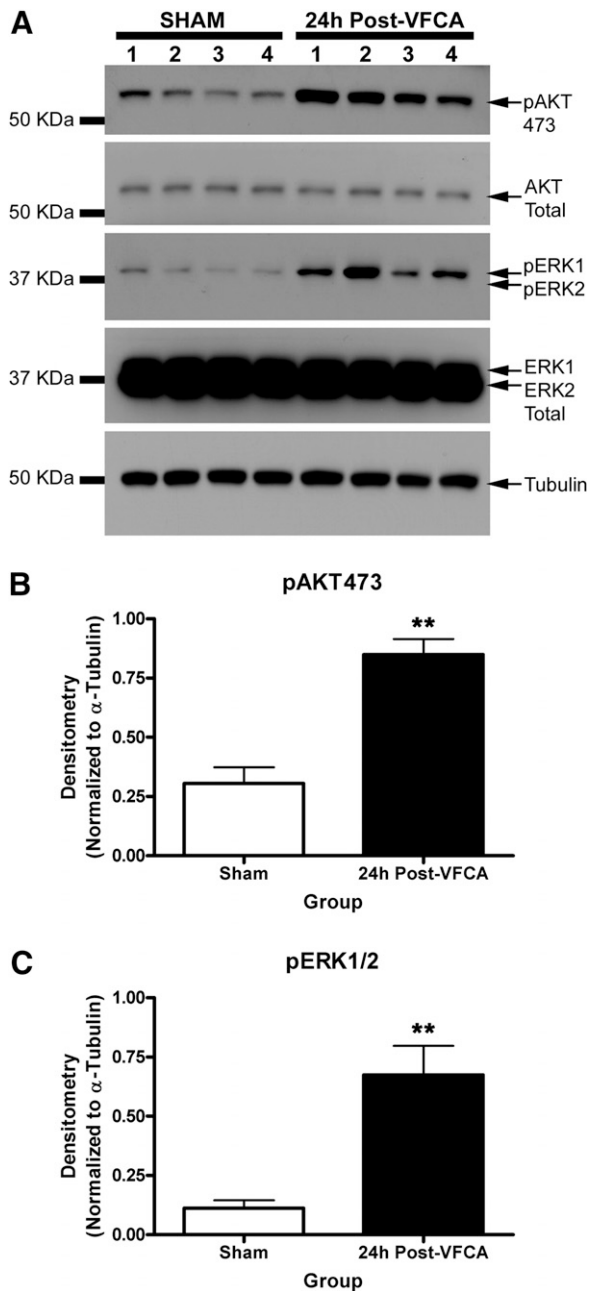
A

B

pAKT473

C

pERK1/2

Fig. 8. Alteration in kinases after cardiac arrest-induced brain ischemia. (A) Western blots show changes in hippocampal pAKT473, AKT Total, pERK1/2, and ERK Total 24 hours after a 6-minute CA (n = 4/group). (B and C) Semiquantitative densitometry showing that pAKT473 and pERK1/2 significantly increase in the hippocampus after CA (n = 4/group). Data were analyzed by unpaired t test. **P < 0.01. Graphs show mean + S.E.M. KDa, kilodalton.

Furthermore, NSC117079 dose-dependently altered astrocyte morphology and reduced viability. In contrast, NSC45586 was not toxic to astrocytes. Their differential potencies for ERK inhibition may explain, in part, divergent effects on viability. ERK is a critical signaling kinase in astrocytes. It is intimately linked to survival, migration, and proliferation (Mandell and VandenBerg, 1999; Takuma et al., 2000; Lim et al., 2007). NSC117079 more potently inhibited ERK, which may have blocked essential survival mechanisms in astrocytes.

We explored whether the unexpected biochemical effects of drug treatment on astrocytes was due to inhibition of novel PHLPP1 and/or PHLPP2 signaling mechanisms. To test this hypothesis, astrocytes were transduced with either PHLPP1 or PHLPP2 targeting vectors. PHLPP1 KD increased AKT but not ERK activation in astrocytes under serum growth conditions (i.e., 10% FBS). This is consistent with work of Chen et al. (2013), who showed that astrocytes isolated from PHLPP1 KO mice had higher AKT but not ERK phosphorylation after acute IGF-1 stimulation.

PHLPP2 KD tended to decrease both AKT and ERK activation—similar to changes induced by PHLPP inhibitors. The results suggest that PHLPP2 promotes (or helps maintain) AKT/ERK phosphorylation in astrocytes. Inhibiting the AKT/ERK pathways in injured astrocytes may exacerbate cell death (Nawashiro et al., 2000; Gabryel et al., 2004). The contribution of the death of astrocytes in brain injury is underappreciated and may be important (Zhao et al., 2003). Because PHLPP1 KD activated AKT in both neurons and astrocytes, selective PHLPP1 inhibitors may be a much safer approach to target cell death in global ischemic brain injury.

The results also reveal an exciting (albeit unintentional) conceptual use for these PHLPP inhibitors. Spinal cord injury is characterized by neuronal death and reactive astrocyte proliferation. A major goal of therapy in that condition is to attenuate neuronal death (i.e., promote survival signaling in neurons) but simultaneously mitigate astrocyte proliferation (i.e., inhibit survival/growth signaling in astrocytes to limit glial scar formation). Thus, these PHLPP inhibitors are prime candidates for testing in spinal cord injury (Ito et al., 2009). The role of the glial scar in ischemic brain injury is less well characterized but could also be important.

PHLPP1 Is a Key Phosphatase in Global Brain Ischemia

The hippocampus is highly vulnerable to damage by transient global ischemia (Horstmann et al., 2010). VF CA is one of the most common causes of transient global brain ischemia in humans and is associated with long-term cognitive deficits in survivors (Mateen et al., 2011). We tested if PHLPPs and their target kinases (AKT and ERK) change in the hippocampus after VF CA-induced ischemic brain injury. AKT and ERK phosphorylation were increased 24 hours after injury. Only PHLPP1 levels significantly increased 24 hours after VF CA. In contrast PHLPP2, PTEN, PP2A, and PP1α did not increase. Rather the latter three phosphatases all significantly decreased, which may have contributed to the increase in AKT/ERK activation. Decreased PP2A activity mediates increased ERK activation in the brain after asphyxia CA in rats (Ho et al., 2007).

We do not yet know whether PHLPP1 protein levels increase predominantly in CA1 and/or at other hippocampal subregions after VF CA (total hippocampal homogenates were used for Western blot analysis in our studies). We also do not know which cell type(s) are involved. Measuring PHLPP1 by immunohistochemistry would normally be an appropriate experiment used to answer these questions. Unfortunately, recent studies show that commercially available PHLPP1 antibodies (including the one used in our work) crossreact with the unrelated protein β-catenin (Lobert et al., 2013). At present, this confounds interpretation and analysis of
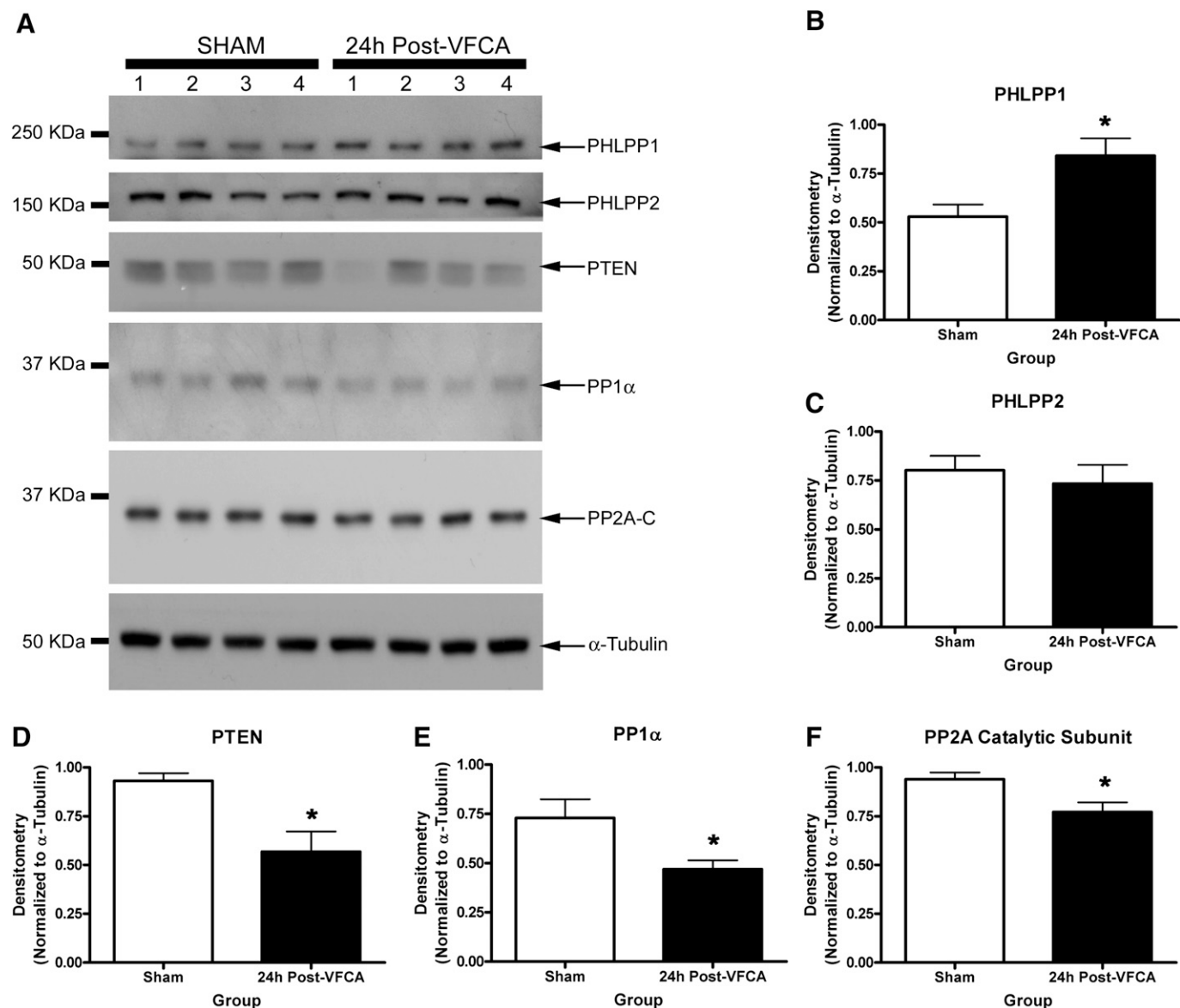
Fig. 9. Alteration in phosphatases after cardiac arrest-induced brain ischemia. (A) Western blots show changes in hippocampal PHLPP1, PHLPP2, PTEN, PP1α, and PP2A 24 hours after a 6-minute CA (n = 4/group). (B) Semiquantitative densitometry showing that PHLPP1 levels significantly increase in the hippocampus after CA (n = 4/group). (C) Semiquantitative densitometry showing that PHLPP2 levels do not change in the hippocampus after CA (n = 4/group). (D–F) Semiquantitative densitometry showing that PTEN, PP1α, and PP2A (catalytic subunit) all significantly decrease in the hippocampus after CA (n = 4/group). Data were analyzed by unpaired t test. *P < 0.05. Graphs show mean + S.E.M. KDa, kilodalton.

PHLPP1 regional/cellular distribution postischemia by immunohistochemistry. We also observed similar crossreactivity using a total of four PHLPP antibodies, precluding the use of immunohistochemical approaches in our studies (data not shown). Nevertheless, future studies should explore whether PHLPP1 upregulation is also induced by in vitro oxygen glucose deprivation. This model may help to distinguish (by Western blot) PHLPP1/AKT signaling changes in neurons, astrocytes, oligodendrocytes, and microglia postischemia.

Our observation that AKT activation is potentiated in the damaged ischemic brain is consistent with other studies (Namura et al., 2000; Endo et al., 2006; Miyawaki et al., 2009); although to the best of our knowledge, we are the first to report increased pAKT in a rat model of VF CA. Furthermore, recent studies found that AKT activation promotes PHLPP1 activity by preventing its degradation (Li et al., 2009), which

may be a feedback loop. Therefore prolonged (24 hour) AKT activation in the VF CA injured hippocampus may cause PHLPP1 levels to increase via this feedback inhibitory mechanism (functioning to switch-off survival signaling). In primary neurons we found that 24 hour IGF-1 stimulation (a potent AKT activator) tended to raise PHLPP1 levels (Supplemental Fig. 6), suggesting that this potential signaling mechanism can be explored in the in vitro setting. Together our results suggest that some phosphatases may decrease activity in the hippocampus after VF CA and promote AKT survival signaling. In contrast, increased PHLPP1 may function to turn-off AKT and promote cell death. Therefore selective PHLPP1 inhibitors could be used to prolong endogenous AKT survival signaling after global brain ischemia (Fig. 10).

Taken together, our mechanistic (in vitro) and observational (ex vivo) findings support the conclusion that
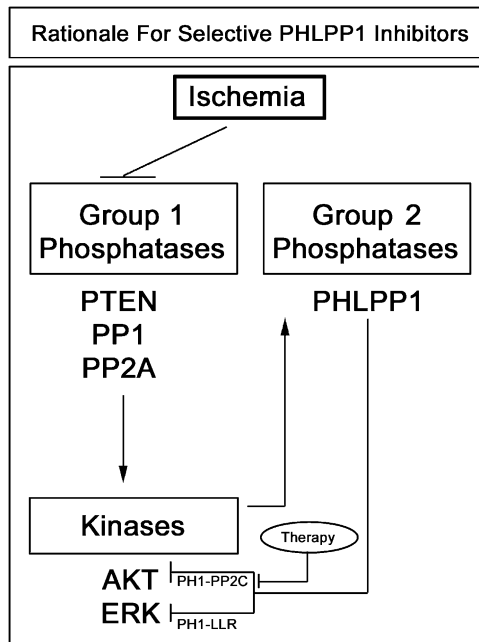
Fig. 10. Potential mechanism of increased PHLPP1 after CA and rationale for developing novel selective (PP2C domain targeting) PHLPP1 inhibitors. Inhibition of brain phosphatases contributes to increased kinase activation after cardiac arrest (Ho et al., 2007). Consistent with prior reports we found that total protein levels of several endogenous AKT/ERK inhibitors (herein referred to as Group 1 Phosphatases) decrease in our model of VF CA-induced brain injury. The decrease in Group 1 phosphatases coincided with increased AKT and ERK phosphorylation. Recent studies show that AKT activation promotes PHLPP1 stabilization and prevents its degradation (Li et al., 2009). Upregulation of Group 2 Phosphatases may function to turn-off kinase activation. PHLPP1 levels significantly increase along with AKT, potentially mediating feedback inhibition. Future development of selective (PP2C domain targeting) PHLPP1 inhibitors may prolong AKT activation after brain ischemia.

proportionally to total protein levels after VF CA. Together the data support the need for further exploration of PHLPP1 as a key therapeutic target in global brain ischemia.

References

Aharon AS, Mulloy MR, Drinkwater DC, Jr, Lao OB, Johnson MD, Thunder M, Yu C, and Chang P (2004) Cerebral activation of mitogen-activated protein kinases after circulatory arrest and low flow cardiopulmonary bypass. *Eur J Cardiothorac Surg* **26:**912–919.

Beiser DG, Wojcik KR, Zhao D, Orbelyan GA, Hamann KJ, and Vanden Hoek TL (2010) Akt1 genetic deficiency limits hypothermia cardioprotection following murine cardiac arrest. *Am J Physiol Heart Circ Physiol* **298:**H1761–H1768.

Bonacci TM, Mathews JL, Yuan C, Lehmann DM, Malik S, Wu D, Font JL, Bidlack JM, and Smrcka AV (2006) Differential targeting of Gbetagamma-subunit signaling with small molecules. *Science* **312:**443–446.

Brewer GJ, Torricelli JR, Evege EK, and Price PJ (1993) Optimized survival of hippocampal neurons in B27-supplemented Neurobasal, a new serum-free medium combination. *J Neurosci Res* **35:**567–576.

Brognard J, Sierecki E, Gao T, and Newton AC (2007) PHLPP and a second isoform, PHLPP2, differentially attenuate the amplitude of Akt signaling by regulating distinct Akt isoforms. *Mol Cell* **25:**917–931.

Chen B, Van Winkle JA, Lyden PD, Brown JH, and Purcell NH (2013) PHLPP1 gene deletion protects the brain from ischemic injury. *J Cereb Blood Flow Metab* **33:** 196–204.

Cho DG, Mulloy MR, Chang PA, Johnson MD, Aharon AS, Robison TA, Buckles TL, Byrne DW, and Drinkwater DC, Jr (2004) Blockade of the extracellular signal-regulated kinase pathway by U0126 attenuates neuronal damage following circulatory arrest. *J Thorac Cardiovasc Surg* **127:**1033–1040.

Clausen F, Lundqvist H, Ekmark S, Lewén A, Ebendal T, and Hillered L (2004) Oxygen free radical-dependent activation of extracellular signal-regulated kinase mediates apoptosis-like cell death after traumatic brain injury. *J Neurotrauma* **21:** 1168–1182.

Dash PK, Mach SA, and Moore AN (2002) The role of extracellular signal-regulated kinase in cognitive and motor deficits following experimental traumatic brain injury. *Neuroscience* **114:**755–767.

Endo H, Nito C, Kamada H, Nishi T, and Chan PH (2006) Activation of the Akt/GSK3beta signaling pathway mediates survival of vulnerable hippocampal neurons after transient global cerebral ischemia in rats. *J Cereb Blood Flow Metab* **26:** 1479–1489.

Fukunaga K and Kawano T (2003) Akt is a molecular target for signal transduction therapy in brain ischemic insult. *J Pharmacol Sci* **92:**317–327.

Gabryel B, Pudelko A, and Malecki A (2004) Erk1/2 and Akt kinases are involved in the protective effect of aniracetam in astrocytes subjected to simulated ischemia in vitro. *Eur J Pharmacol* **494:**111–120.

Gao T, Furnari F, and Newton AC (2005) PHLPP: a phosphatase that directly dephosphorylates Akt, promotes apoptosis, and suppresses tumor growth. *Mol Cell* **18:**13–24.

Ho Y, Logue E, Callaway CW, and DeFranco DB (2007) Different mechanisms account for extracellular-signal regulated kinase activation in distinct brain regions following global ischemia and reperfusion. *Neuroscience* **145:**248–255.

Horstmann A, Frisch S, Jentzsch RT, Müller K, Villringer A, and Schroeter ML (2010) Resuscitating the heart but losing the brain: brain atrophy in the aftermath of cardiac arrest. *Neurology* **74:**306–312.

Isaeva E, Lushnikova I, Savrasova A, Skibo G, Holmes GL, and Isaev D (2010) Blockade of endogenous neuraminidase leads to an increase of neuronal excitability and activity-dependent synaptogenesis in the rat hippocampus. *Eur J Neurosci* **32:**1889–1896.

Ito M, Natsume A, Takeuchi H, Shimato S, Ohno M, Wakabayashi T, and Yoshida J (2009) Type I interferon inhibits astrocytic gliosis and promotes functional recovery after spinal cord injury by deactivation of the MEK/ERK pathway. *J Neurotrauma* **26:**41–53.

Jackson TC, Rani A, Kumar A, and Foster TC (2009) Regional hippocampal differences in AKT survival signaling across the lifespan: implications for CA1 vulnerability with aging. *Cell Death Differ* **16:**439–448.

Jackson TC, Verrier JD, and Kochanek PM (2013) Anthraquinone-2-sulfonic acid (AQ2S) is a novel neurotherapeutic agent. *Cell Death Dis* **4:**e451.

Jackson TC, Verrier JD, Semple-Rowland S, Kumar A, and Foster TC (2010) PHLPP1 splice variants differentially regulate AKT and PKCα signaling in hippocampal neurons: characterization of PHLPP proteins in the adult hippocampus. *J Neurochem* **115:**941–955.

pharmacological PHLPP targeting strategies (to treat ischemic brain injury) might be optimized by developing selective PHLPP1 inhibitors. Selective PHLPP1-PP2C inhibitors may be advantageous because 1) they will activate prosurvival AKT signaling in both neurons and astrocytes (Fig. 7F) but 2) avoid interrupting with PHLPP-mediated ERK inhibition in neurons, which limits prodeath ERK activation after VF CA (Fig. 10). This concept is further supported by recent studies showing that hypoxic preconditioning protects against global brain ischemia by simultaneously activating AKT while inhibiting ERK (Zhan et al., 2012). Finally, prior studies in mice found that PHLPP1 overexpression in the hippocampus worsened performance on a learning and memory task (Shimizu et al., 2007). Thus, our novel findings on increased PHLPP1 expression in the brain postinjury also suggest a potential approach to improve cognitive recovery (independent of neuronal death).

In summary, here we show for the first time that several PHLPP inhibitors activate AKT in primary neurons but inhibit it in astrocytes. Because PHLPP1 KD activates AKT both in neurons and astrocytes, future studies should focus on the development of highly selective PHLPP1 inhibitors. Finally, PHLPP1 levels increased in the hippocampus after VF CA-induced injury, which may serve to limit endogenous AKT neuroprotective mechanisms. Future studies are needed to explore if PHLPP1-PP2C catalytic activity increases

Janata A, Magnet IA, Drabek T, Stezoski JP, Janesko-Feldman K, Popp E, Garman RH, Tisherman SA, and Kochanek PM (2013) Extracorporeal Versus Conventional Cardiopulmonary Resuscitation After Ventricular Fibrillation Cardiac Arrest in Rats: A Feasibility Trial. *Crit Care Med* **41**:e211–e222.

Jo H, Mondal S, Tan D, Nagata E, Takizawa S, Sharma AK, Hou Q, Shanmugasundaram K, Prasad A, and Tung JK, et al. (2012) Small molecule-induced cytosolic activation of protein kinase Akt rescues ischemia-elicited neuronal death. *Proc Natl Acad Sci USA* **109**:10581–10586.

Li X, Liu J, and Gao T (2009) beta-TrCP-mediated ubiquitination and degradation of PHLPP1 are negatively regulated by Akt. *Mol Cell Biol* **29**:6192–6205.

Lim JH, Gibbons HM, O'Carroll SJ, Narayan PJ, Faull RL, and Dragunow M (2007) Extracellular signal-regulated kinase involvement in human astrocyte migration. *Brain Res* **1164**:1–13.

Lin YC, Huang ZH, Jan IS, Yeh CC, Wu HJ, Chou YC, and Chang YC (2002) Development of excitatory synapses in cultured neurons dissociated from the cortices of rat embryos and rat pups at birth. *J Neurosci Res* **67**:484–493.

Lobert VH, Bruun J, Abrahamsen H, Lothe RA, Stenmark H, Kolberg M, and Campsteijn C (2013) Antibody crossreactivity between the tumour suppressor PHLPP1 and the proto-oncogene β-catenin. *EMBO Rep* **14**:10–11.

Lu K, Liang CL, Liliang PC, Yang CH, Cho CL, Weng HC, Tsai YD, Wang KW, and Chen HJ (2010) Inhibition of extracellular signal-regulated kinases 1/2 provides neuroprotection in spinal cord ischemia/reperfusion injury in rats: relationship with the nuclear factor-kappaB-regulated anti-apoptotic mechanisms. *J Neurochem* **114**:237–246.

Lu KT, Wang YW, Wo YY, and Yang YL (2005) Extracellular signal-regulated kinase-mediated IL-1-induced cortical neuron damage during traumatic brain injury. *Neurosci Lett* **386**:40–45.

Luo HR, Hattori H, Hossain MA, Hester L, Huang Y, Lee-Kwon W, Donowitz M, Nagata E, and Snyder SH (2003) Akt as a mediator of cell death. *Proc Natl Acad Sci USA* **100**:11712–11717.

Mai BK, Viet MH, and Li MS (2010) Top leads for swine influenza A/H1N1 virus revealed by steered molecular dynamics approach. *J Chem Inf Model* **50**:2236–2247.

Mandell JW and VandenBerg SR (1999) ERK/MAP kinase is chronically activated in human reactive astrocytes. *Neuroreport* **10**:3567–3572.

Mateen FJ, Josephs KA, Trenerry MR, Felmlee-Devine MD, Weaver AL, Carone M, and White RD (2011) Long-term cognitive outcomes following out-of-hospital cardiac arrest: a population-based study. *Neurology* **77**:1438–1445.

Miyawaki T, Ofengeim D, Noh KM, Latuszek-Barrantes A, Hemmings BA, Follenzi A, and Zukin RS (2009) The endogenous inhibitor of Akt, CTMP, is critical to ischemia-induced neuronal death. *Nat Neurosci* **12**:618–626.

Murga C, Laguinge L, Wetzker R, Cuadrado A, and Gutkind JS (1998) Activation of Akt/protein kinase B by G protein-coupled receptors. A role for alpha and beta gamma subunits of heterotrimeric G proteins acting through phosphatidylinositol-3-OH kinasegamma. *J Biol Chem* **273**:19080–19085.

Namura S, Nagata I, Kikuchi H, Andreucci M, and Alessandrini A (2000) Serine-threonine protein kinase Akt does not mediate ischemic tolerance after global ischemia in the gerbil. *J Cereb Blood Flow Metab* **20**:1301–1305.

Nawashiro H, Brenner M, Fukui S, Shima K, and Hallenbeck JM(2000) High susceptibility to cerebral ischemia in GFAP-null mice. *J Cereb Blood Flow Metab* **20**:1040–1044.

Ozawa H, Shioda S, Dohi K, Matsumoto H, Mizushima H, Zhou CJ, Funahashi H, Nakai Y, Nakajo S, and Matsumoto K (1999) Delayed neuronal cell death in the rat hippocampus is mediated by the mitogen-activated protein kinase signal transduction pathway. *Neurosci Lett* **262**:57–60.

Raghupathi R, Muir JK, Fulp CT, Pittman RN, and McIntosh TK (2003) Acute activation of mitogen-activated protein kinases following traumatic brain injury in the rat: implications for posttraumatic cell death. *Exp Neurol* **183**:438–448.

Schwindinger WF and Robishaw JD (2001) Heterotrimeric G-protein betagamma-dimers in growth and differentiation. *Oncogene* **20**:1653–1660.

Shimizu K, Okada M, Nagai K, and Fukada Y (2003) Suprachiasmatic nucleus circadian oscillatory protein, a novel binding partner of K-Ras in the membrane rafts, negatively regulates MAPK pathway. *J Biol Chem* **278**:14920–14925.

Shimizu K, Okada M, Takano A, and Nagai K (1999) SCOP, a novel gene product expressed in a circadian manner in rat suprachiasmatic nucleus. *FEBS Lett* **458**:363–369.

Shimizu K, Phan T, Mansuy IM, and Storm DR (2007) Proteolytic degradation of SCOP in the hippocampus contributes to activation of MAP kinase and memory. *Cell* **128**:1219–1229.

Sierecki E, Sinko W, McCammon JA, and Newton AC (2010) Discovery of small molecule inhibitors of the PH domain leucine-rich repeat protein phosphatase (PHLPP) by chemical and virtual screening. *J Med Chem* **53**:6899–6911.

Takuma K, Fujita T, Kimura Y, Tanabe M, Yamamuro A, Lee E, Mori K, Koyama Y, Baba A, and Matsuda T (2000) T-588 inhibits astrocyte apoptosis via mitogen-activated protein kinase signal pathway. *Eur J Pharmacol* **399**:1–8.

Verrier JD, Exo JL, Jackson TC, Ren J, Gillespie DG, Dubey RK, Kochanek PM, and Jackson EK (2011) Expression of the 2′,3′-cAMP-adenosine pathway in astrocytes and microglia. *J Neurochem* **118**:979–987.

Zhan L, Li D, Liang D, Wu B, Zhu P, Wang Y, Sun W, and Xu E (2012) Activation of Akt/FoxO and inactivation of MEK/ERK pathways contribute to induction of neuroprotection against transient global cerebral ischemia by delayed hypoxic postconditioning in adult rats. *Neuropharmacology* **63**:873–882.

Zhao X, Ahram A, Berman RF, Muizelaar JP, and Lyeth BG (2003) Early loss of astrocytes after experimental traumatic brain injury. *Glia* **44**:140–152.

Address correspondence to: Patrick M. Kochanek, University of Pittsburgh, School of Medicine, Department of Critical Care Medicine, Safar Center for Resuscitation Research, 3434 Fifth Avenue, Pittsburgh, PA 15260. E-mail: kochanekpm@ccm.upmc.edu